ELSEVIER

A hydrologically driven model of swamp water mosquito population dynamics

Jeffrey Shaman[a,*], *Marc Spiegelman*[b], *Mark Cane*[b], *Marc Stieglitz*[c]

[a] *College of Oceanic and Atmospheric Sciences, 104 COAS Admin Bldg., Oregon State University, Corvallis, OR 97331, USA*
[b] *Department of Earth and Environmental Sciences, Columbia University, USA*
[c] *Department of Civil and Environmental Engineering, Georgia Institute of Technology, GA, USA*

ABSTRACT

We develop a swamp water mosquito population model that is forced solely by environmental variability. Measured temperature and land surface wetness conditions are used to simulate *Anopheles walkeri* population dynamics in a northern New Jersey habitat. Land surface wetness conditions, which represent oviposition habitat availability, are derived from simulations using a dynamic hydrology model. Using only these two density-independent effects, population model simulations of biting *Anoph. walkeri* correlate significantly with light trap collections. These results suggest that prediction of mosquito populations and the diseases they transmit could be better constrained by inclusion of environmental variability.

1. Introduction

Over the last 50 years, many models describing insect population variability have been developed. Many of these models have been designed to account for density-dependent effects, including predator–prey and host–pathogen interactions. Traditionally, density-independent effects have been treated either as noise (May, 1986, and its citations) or within regularly varying theoretical frameworks, such as by using oscillatory equations to represent variable carrying capacity (Nisbet and Gurney, 1976; Cushing, 1986).

The model presented here accounts for two density-independent factors, temperature and the availability of mosquito breeding habitats. We examine whether these variables, when applied to a simple population model, describe some of the observed mosquito population variability. Fluctuations of habitat availability are determined by modeled surface wetness as simulated by a dynamic hydrology model. Previously, such model simulations have been used to describe the emergence of flood and swamp water mosquitoes in a New Jersey habitat (Shaman et al., 2002). Here, we couple these simulations with a mosquito life cycle model. In doing so, real environmental variability is expressed within the model through variation in the availability of breeding habitats. The effects of temperature on mosquito developmental rates are also accounted for. Modeling this way allows

for complex, realistic treatment of these density-independent effects for this New Jersey mosquito population. We will show that these density-independent effects, i.e. environmental variability, can produce modeled mosquito population variability consistent with observed mosquito population dynamics.

2. Methods

The hydrology model employed for this study (Stieglitz et al., 1997) has been applied to two northern New Jersey watersheds, and positive associations of model predicted surface wetness and mosquito collection abundance have been established for both flood and swamp water species (Shaman et al., 2002). These findings are consistent with the biology of these mosquito species: with more surface wetness, more breeding habitats are available such that mosquito reproduction and larval survival are favored. In effect, increased surface wetness supports a greater flood and swamp water mosquito population.

For this study, we focus on the adult mosquito population record collected by New Jersey light trap at the Great Swamp National Wildlife Refuge, Morris County, New Jersey. This 15-year record from the summer months was collected in an area without mosquito control and provides a relatively undisturbed record of the populations of certain mosquito species. Fig. 1 shows the 15-year record for the swamp water species *Anopheles walkeri*.

2.1. Mosquito biology

The life cycle of the mosquito begins as an egg, which given the right conditions hatches as a larvae. The larvae develop through several instar stages before entering pupation. After pupation, the mosquito emerges as an adult. Adults generally mate within the first few hours of emergence; females then seek a blood meal to provide a protein source for their eggs. After biting, the female rests while her eggs develop. Once fully developed, the female oviposits and then proceeds to find another blood meal and repeat the gonotrophic cycle.

Temperature and the availability of appropriate aquatic breeding habitats are the two environmental variables that most impact the abundance of mosquitoes (Kettle, 1995). Temperature impacts both the survivorship and developmental rate of mosquitoes; surface wetness, as mentioned above, limits the population size of sub-adult mosquitoes. These two parameters, temperature and surface wetness, will be used to force the model mosquito population.

2.2. Model description

For the purposes of this work, the mosquito life cycle will proceed continuously—no overwinterings, no diapause, no hibernation, no breaks in the reproductive cycle. The system will presume that eggs are deposited directly on breeding waters and immediately proceed through development, which is consistent with the biology of the swamp water species *Anoph. walkeri*. The first three stages of the life cycle—egg, larvae
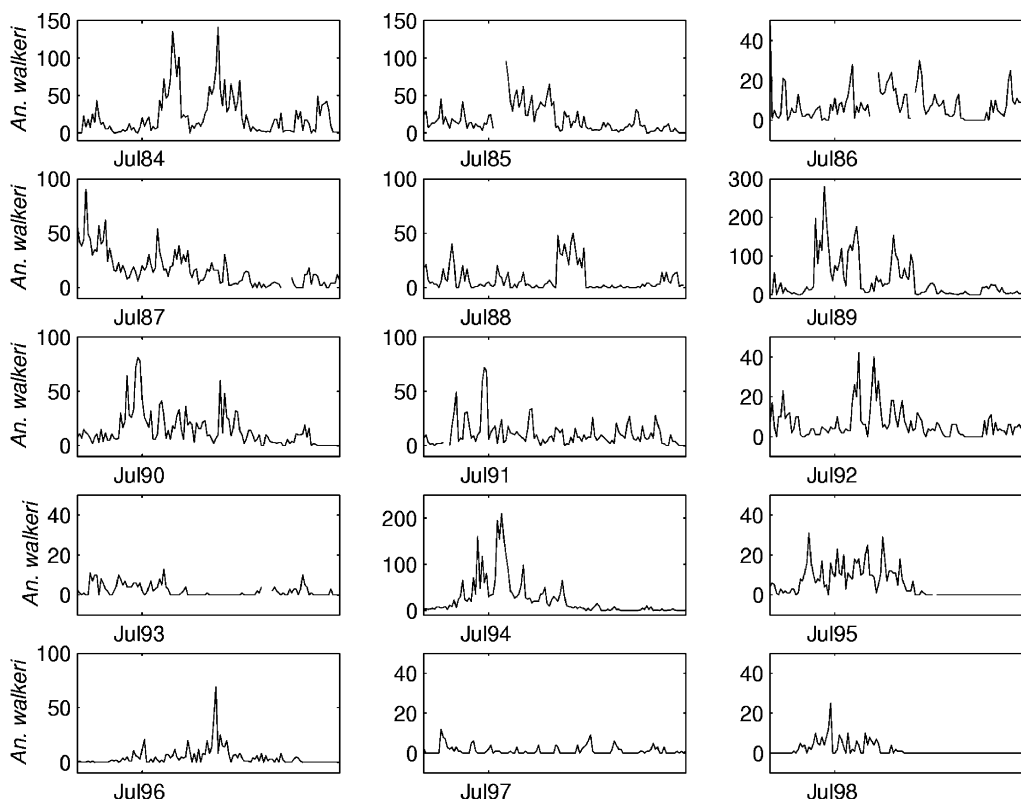

Fig. 1 – Time series of the June–September 1984–1998 daily New Jersey light trap collections of *Anopheles walkeri* in the Great Swamp National Wildlife Refuge. Note the different scales for different years.

and pupae—will be lumped into one aquatic population (also called larvae). The adult population will be linked but monitored separately. Only female mosquitoes will be modeled.

The model is designed as follows. The mosquitoes are assumed to live no more than 40 days. A suite of 40 population cohorts is tracked through real time. Each cohort represents a group of mosquitoes oviposited on the same day, and each cohort possesses a development time, distinct from real time, that determines where in the mosquito life cycle the cohort resides. The cohort populations diminish through real time by a temperature-dependent mortality rate (discussed below). Emergent and reproductive 'events' are determined by the respective times of development (also discussed below). Forty days of life are monitored, after which all the mosquitoes are presumed to have died.

2.3. Mortality and survivorship

Survival for both the aquatic and adult populations is assumed to follow a simple exponential function:

$$\frac{d\Gamma(t, t_0)}{dt} = -r\Gamma(t, t_0) \tag{1}$$

$$\frac{dN(t, t_0)}{dt} = -rN(t, t_0)$$

$$\text{if } t - t_0 \geq 40, \quad \text{then } \Gamma(t, t_0) = N(t, t_0) = 0$$

where $\Gamma(t, t_0)$ is the cohort of larvae at real time t, born on day, t_0, $N(t, t_0)$ the cohort of adults born on day, t_0 and r is the mortality rate. The mortality rate varies as an empirically derived function of temperature (Martens, 1997):

$$r = \left(-4.4 + 1.31 \times T - 0.03 \times T^2\right)^{-1} \tag{2}$$

where T is the temperature in degrees C, and r^{-1} is in units of time.

2.4. Development of the aquatic population

The total development time of a mosquito through its sub-adult stages varies as a function of temperature, ranging from 7 to 20 days, depending on the species. Empirical functions describing this developmental relationship generally take the following form (Craig et al., 1999):

$$\frac{d\tau(t, t_0)}{dt} = \frac{T - T_e}{\text{TDD}_e} \tag{3}$$

where $\tau(t, t_0)$ is the aquatic development time for the cohort of larvae born on day, t_0, T the mean daily temperature in degrees Celsius, T_e the minimum temperature at which the larvae can survive and TDD_e is the total degree days for emergence, i.e. the number of degrees, measured on a daily basis, required before the larvae will be fully developed to the adult stage. Once an aquatic population reaches a total τ of one, the population emerges as adults, i.e.:

$$N(t, t_0) = \Gamma(t, t_0) \times H(\tau(t, t_0) - 1) \tag{4}$$

where H is the Heaviside function ($H(x) = 0$ if $x \leq 0$; $H(x) = 1$, if $x > 0$).

2.5. Development in the adult population

An identical function then tracks the life cycle of each adult cohort, such that:

$$\frac{d\Phi(t, t_0)}{dt} = \frac{T - T_o}{\text{TDD}_o} \tag{5}$$

where $\Phi(t, t_0)$ is the development time of the eggs carried by the adult cohort born on day, t_0, T_o the minimum temperature at which the adults can survive and TDD_o is the total degree days for oviposition. When Φ reaches one, the eggs are lain and Φ is reset to zero. The adults can proceed through as many gonotrophic cycles as time (a maximum of 40 days of life) and temperature (Φ is a function of temperature) permit. On each day t the number of eggs oviposited is given by:

$$\Gamma(t, t_0) = b \times \sum \{N(t, t_0) \times H(\Phi(t, t_0) - 1)\} \tag{6}$$

Thus, the number of eggs produced on a given day equals the total number of adults reaching $\Phi = 1$ on that day times a reproductive rate, b. More than one cohort of adults may oviposit on a particular day, as development rates will vary if temperature has varied. A single adult cohort may reproduce more than once in its lifetime; the reproductive cycle is reset for an adult cohort after oviposition, i.e.:

$$\text{if } \Phi(t, t_0) \geq 1, \quad \text{then } \Phi(t, t_0) = 0 \tag{7}$$

3. Modeling the system

3.1. Testing the model

With a maximum lifespan of 40 days, 40 discrete population cohorts need to be tracked at any given time (i.e. the mosquito population that is 2 days old, the mosquito population that is 3 days old, etc.). Thus, the system is 40-coupled ODEs. The core of this model is the balance of the mortality function and reproductive growth. For model calibration, we began by assuming an average time of development of 10 days, a T_e and T_o of 14 °C, and a mean temperature of 24 °C. These parameters require a TDD_e and TDD_o of 100 °C. If temperature, T, is held constant, fixed points – steady-states of equal birth and death and no change through time of the population structure – will exist. With $T = 24$ °C, a reproductive rate $b = 5.7114$ produces such a fixed point solution, i.e. the population neither increases nor decreases (see Appendix A for details). This steady-state model solution was used to test the accuracy of various stepping algorithms for use in running the numeric model. A fourth-order Runga–Kutta scheme was found to be stable and is employed here.

3.2. Fluctuations in temperature

The response of the model to variations in temperature was examined next. A sinusoidal function for temperature with a
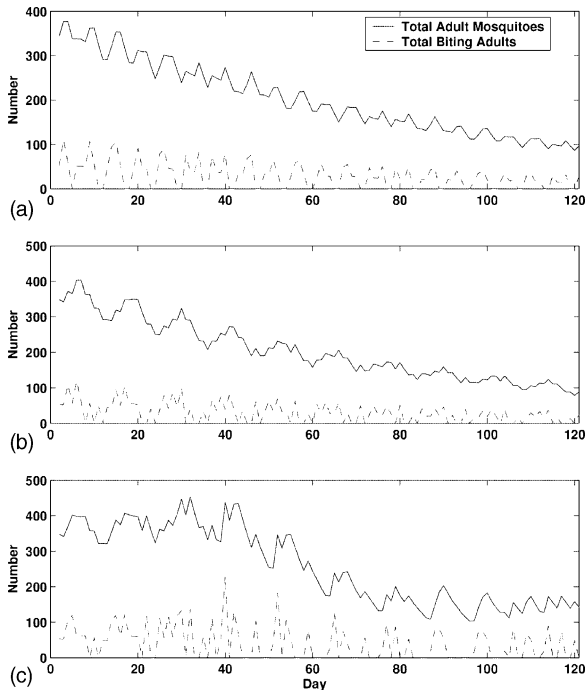
(a)

(b)

(c)

Fig. 2 – (a) Time series from a 120-day run of the model with $T = 24 + 6 \times \sin(2\pi \times t/6)$, $b = 5.7114$. Shown are the total numbers of adult mosquitoes on each day (sum of all cohorts), and the number of biting mosquitoes (new emergents and parous adults that have just oviposited). (b) Same as (a), but for $T = 24 + 6 \times \sin(2\pi \times t/12)$. (c) Same as (a), but for $T = 24 + 6 \times \sin(2\pi \times t/12) + 2 \times \sin(2\pi \times t/80)$.

Fig. 3 – Same as **Fig. 2**c, but for $b = 10$.

period of 6 days was chosen, $T = 24 + 6 \times \sin(2\pi \times t/6)$. The time step used in the integration was 1 h (0.0417 days). The temperature function, while not mimicking weather variability, provided a mean temperature of 24 °C for the duration of the run and a range of 18–30 °C. The mean times of development, τ and Φ, remain at 10 days, but individual populations can mature at faster and slower rates depending on the timing of their birth in relation to the temperature function. This variability in time of development was expected to produce convergence of population cohort times of development. In addition, variations in temperature alter mortality rates, which affects reproduction rates.

Fig. 2a shows some of the results from a 120-day run of the model for these conditions. The system does in fact behave as predicted. Periodicities in the population have been generated with only a modest steady-state reproductive rate of 5.7114 (well below the 50–75 females an ovipositing adult produces per brood), and the overall population is in decline. Even greater variability in the population can be generated simply by lengthening the period of the temperature function. Fig. 2b shows such an instance, in which $T = 24 + 6 \times \sin(2\pi \times t/12)$. Twelve day cycles are evident in the population, matching the period of the temperature function. Fig. 2c shows the results of a run with a more complicated function for temperature, $T = 24 + 6 \times \sin(2\pi \times t/12) + 2 \times \sin(2\pi \times t/80)$. Again, the period of the temperature function is apparent in the changes of the total population over the course of the model run.
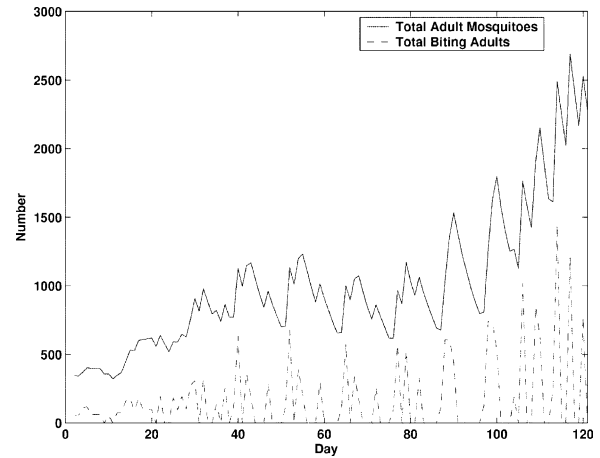
3.3. A higher birth rate

The reproductive rate, b, was raised to 10, not a more realistic number, but one that changes the steady-state, fixed point solution. The model was run with this reproductive rate, the double sinusoid temperature function of Fig. 2c, and the same initial population structure as previous runs. Since the reproductive rate is much higher, the population was expected to climb. Fig. 3 shows that indeed a climb in population results; in fact, the total population swells to enormous numbers; with a realistic birth rate of 50–75 the population would climb even faster. Clearly, something must constrain the population size. Within the model this is where modeled breeding habitat availability comes into play.

3.4. Environmental capacity—linking the population to hydrologic variability

Since surface wetness can be modeled in space and time and a link between surface wetness and mosquito abundance has been established (Shaman et al., 2002), we wish to include these effects in the model. It has been shown that with more surface pooling greater numbers of larvae can survive, and higher number of adult *Anoph. walkeri* are likely to be collected in light traps in northern New Jersey. For the purposes of this model it will be assumed that the impact of drier conditions is to reduce the maximum population size of the larval cohorts.

In standard logistic growth, carrying capacity, K, is a density-dependent modifier of population growth rates. Here, we instead use environmental variability, i.e. surface wetness, as a density-independent constraint on total population size. To avoid any confusion, we therefore define a new variable, environmental capacity, E, to represent the effect of surface wetness conditions on total population size. Many functions could be adopted to account for this constraint—we have used the following: at the end of each day, the total number of larvae is tallied; if this number, N, exceeds that day's environmental capacity, E, each larval population cohort is reduced by the factor E/N. This results in a proportional reduction of each cohort; a cohort comprising 30% of the total larval population before reduction will comprise 30% of the reduced total larval popu-
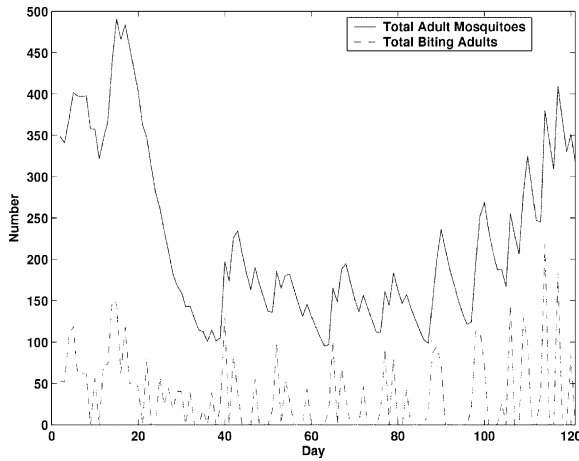
Fig. 4 – Same as Fig. 3, but for $E = 1000 + 600 \times \cos(2\pi \times t/50)$.
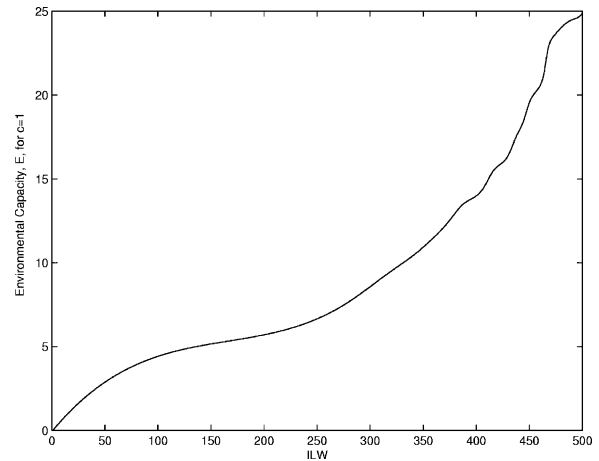

Fig. 5 – Environmental capacity, E, as a function of the index of local wetness (ILW). The function is a cubic spline fitting of the discrete values of $ILW(p_i(0.5))$ (ILW corresponding to a 50% probability for mosquito population size i, found by logistic regression of the mosquito population on the ILW).

lation. This system is by no means an accurate representation of the effects of limited habitat availability, but will be used here as a first approximation.

We first show use of this environmental capacity limitation in an idealized model run. Fig. 4 shows the results of a model run with the same conditions as the previously described run plus the environmental capacity, $E = 1000 + 600 \cos(2\pi \times t/50)$. The population no longer increases without bound but instead oscillates irregularly. Surgings and crashings of both the total and host-seeking populations are apparent, in a fashion qualitatively similar to some of the collection data (Fig. 1).

Simulations were also performed to test model sensitivity to initial conditions. With large enough reproductive rates for a given amplitude E, the model quickly converged to the same solution.

3.5. Incorporating local hydrologic variability

To employ the hydrologic conditions as simulated at the Great Swamp, we have to establish an explicit relationship between local modeled wetness (described and referred to as the index of local wetness, or ILW, in Shaman et al., 2002) and environmental capacity. In this study, we used polytonomous logistic regression, as in Shaman et al. (2002), to establish associations between the ILW and the probability of exceeding 24 discrete populations sizes of *Anoph. walkeri*. Thus, for each of the 24 population categories, an empirical model describing the probability of such a population size given the ILW was derived. The empirical relationship between ILW and environmental capacity was then determined from these models. Logistic regression model probabilities of 50% for all population categories were then selected and used to establish an empirical relationship between increasing wetness and increasing population size (i.e. ILW corresponding to a $p(0.5)$ of each population size or greater being collected). These values were then scaled linearly, such that

$$E_i = c \times ILW(p_i(0.5)) \qquad (8)$$

where c is a scaling constant, the subscript i denotes one of the 24 population sizes used in the logistic regression, $ILW(p_i(0.5))$

the ILW corresponding to a 50% probability for the population size i and E_i is the discrete environmental capacity value for a given wetness. The continuous function for environmental capacity, E, was found by cubic interpolation of the discrete values, E_i, and a bias correction to keep the lowest ILW values positive. The function is somewhat non-linear. Fig. 5 shows this function for $c = 1$.

The scaling constant, c, can be removed from the system of equations by setting $N = cN'$, $\Gamma = c\Gamma'$ and $E = cE'$ and substituting these into Eqs. (1), (4), (6) and (8) to obtain equations for N', Γ' and E'. Note that these new equations have exactly the same form as Eqs. (1), (4), (6) and (8). Therefore, c acts only to scale the size of the model population.

3.6. Real temperature

Hourly temperature data for the area were assembled from National Climate Data Center archives for nearby Allentown, PA. The hourly temperature data ranges from 7 to 38 °C with a mean of approximately 21. These data had also been used in the forcing of the hydrology model (see Shaman et al., 2002).

4. Results

As constructed, the mosquito population model has five parameters: mortality (Eq. (2), $r(T)$); larval development (Eq. (3), $d\tau/dt$); gonotrophic development (Eq. (5), $d\Phi/dt$); the reproductive rate (b); and the scheme for inclusion of environmental capacity (E). Both Eqs. (3) and (5) are themselves the function of two parameters that determine rates of development, i.e. the number of temperature degree-days needed for emergence and ovipositioning, respectively. Specifically, larval development (Eq. (3)) is a function of TDD_e and T_e; gonotrophic development (Eq. (5)) is a function of TDD_o and T_o. Either of these parameters can be varied to lengthen or shorten these rates of development.

To test the sensitivity of the model we explored its parameter space. We varied b, TDD_e and TDD_o, running 2250 simulations, each with a different combination of these parameters. We did not vary the mortality rate, which is empirically derived, or the scheme for inclusion of E. Birth rates were varied from 15 to 105; because we only track females, these numbers provide a biologically realistic range of reproductive rates. TDD_e was varied from 70 to 210, which for a T_e held at 7 °C represents larval development in 5–15 days (if temperature were held fixed at 21 °C, which it was not). Similarly, TDD_o

was varied from 70 to 210, which for a T_o held at 7 °C represents larval development in 5–15 days (if temperature were held fixed at 21 °C, which it was not). Table 1 presents a list of the parameter values employed for model simulations.

Fig. 6 presents the results of these model simulations. These 2250 simulations show that many parameter combinations produce simulations of similar fidelity, and thus demonstrate some degree of model insensitivity to variations of TDD_e, TDD_o and b. In many of the panels of Fig. 6, a pattern emerges equivalent to the contour lines $TDD_o = -TDD_e + a$
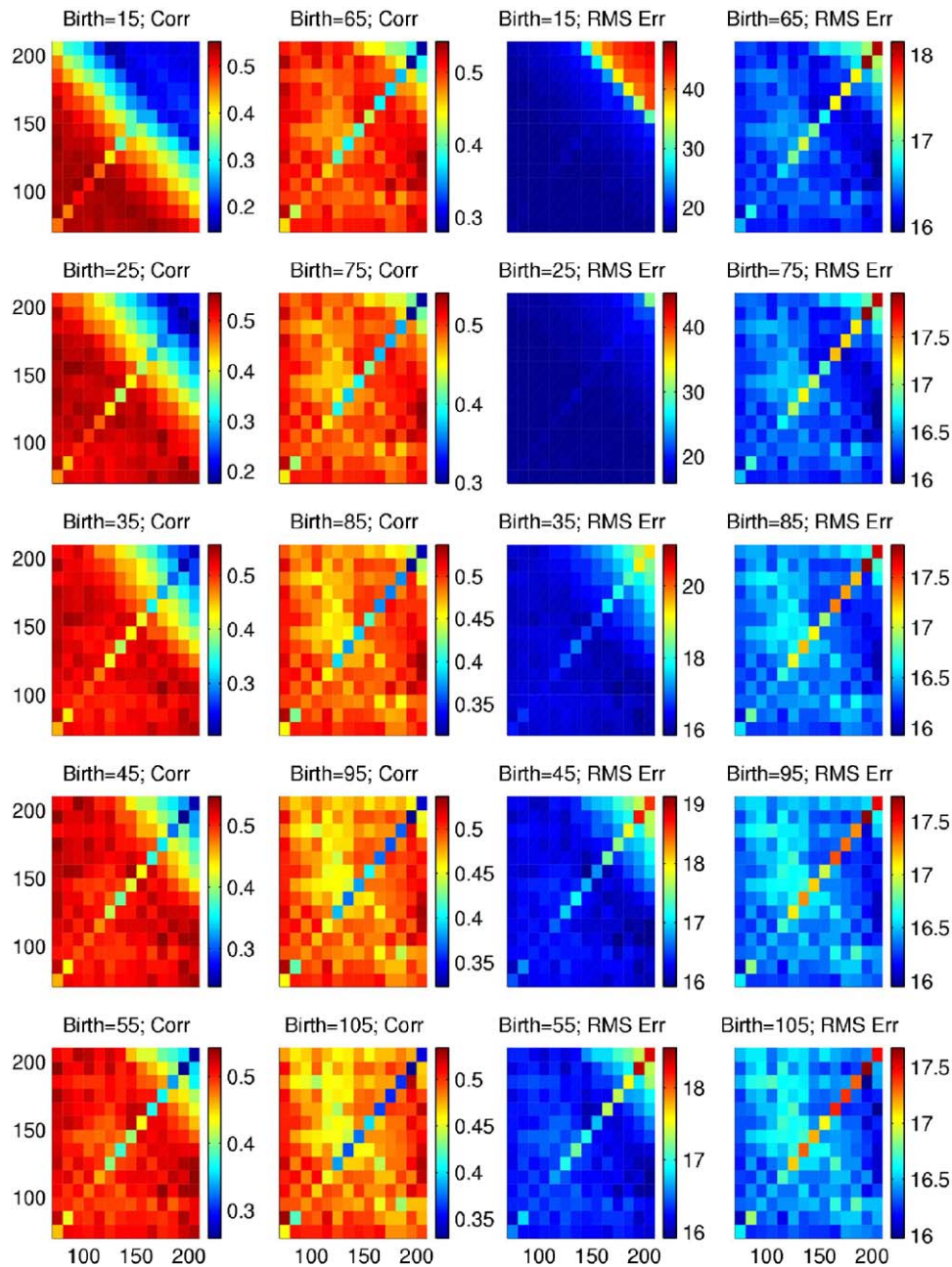

Fig. 6 – Correlation coefficient and RMS error for the 2250 model simulations with the parameters b, TDD_e and TDD_o varied. The left two columns show correlation coefficients, the right two columns present RMS errors. In each plot, the x-axis, TDD_e, varies from 70 to 210 and the y-axis, TDD_o, similarly varies from 70 to 210. Each plot presents a different reproductive rate, b, as labeled.

Table 1 – Parameter values employed in model simulations	
Parameter	Value
b	15–105
TDD_e	70–210
T_e	7
TDD_o	70–210
T_o	7

Mortality, r, is drived from Eq. (2); environmental carrying capacity, E, is derived from Eq. (8); temperature is from the measured record.

(a)

(b)

(c)

Fig. 7 – (a) Model and measured host-seeking (biting) *Anopheles walkeri*. The model simulation is Run 1, as listed in Table 2. (b) Concurrent mean daily temperature; (c) environmental capacity, E.

constant. This suggests that it is the total time of development from egg to oviposition ($TDD_o + TDD_e$) that is critical for accurate model simulation, but how that time is divided between the larval and adult stages is not important. Correlations fall off and RMS errors rise with longer larval and gonotrophic developmental rates, provided that birth rates remain low. There is also a peculiar degradation of model behavior along the line $TDD_o = TDD_e$. Fig. 6 indicates that good model performance occurs when the birth rate is low but the life cycle fast, or if the birth rate is high but the life cycle slow.

Table 2 presents the results for the best-fit model simulations. Shown are the run number, the years of simulation, parameters, the daily correlation with the New Jersey light trap collection data (representative of the host-seeking mosquito population), correlation with a 7-day smoothing applied and the root mean-square (RMS) error with a 7-day smoothing applied. The correlations for these best-fit simulations are highly statistically significant ($p < 0.00001$). Comparison of Run 1 with Run 2 reveals that the model better captures collected *Anoph. walkeri* dynamics for some portions of the record. These results also suggest that for some periods of time habitat availability provides a strong constraint on population dynamics.

Fig. 7 shows the time series of modeled biting adults from Run 1 and of the collection data, each with a 7-day smoothing. Over 56% of the measured variance is explained by the population model. Generally, more extreme events, both population lows, such as the low *Anoph. walkeri* numbers at the end of each season when conditions have dried, and populations spikes, such as the high *Anoph. walkeri* numbers during the 1989 season, are better represented. Fig. 8 presents a similar time series for Run 2. Over this longer period, the model sim-
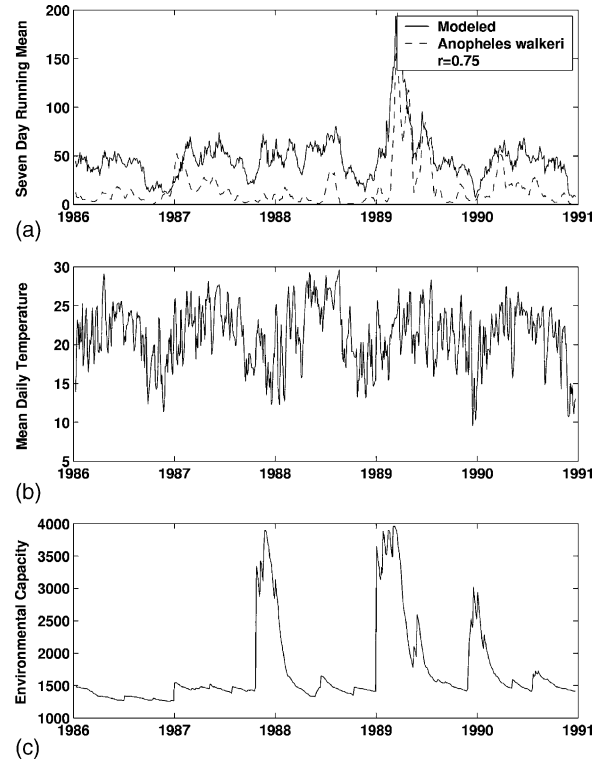
ulations perform less reliably. In particular, the model fails to capture much of the population dynamics from 1993 onward.

Runs 3 and 4 (Table 2) demonstrate the importance of environmental capacity and temperature for producing an accurate model simulation. Changes to these variables (such as replacement of one with a sinusoid or constant) lead to greatly reduced correlation with the collected *Anoph. walkeri* record. For instance, model simulation with constant E and real T (Run 3) yields a weekly correlation coefficient of $r = 0.31$ over whole 15-year record and a daily correlation coefficient of $r = 0.16$. Similarly, model simulation with E as determined by Eq. (8), but constant T (Run 4) yields correlation coefficients of $r = 0.34$ (weekly) $r = 0.27$ (daily).

Table 2 – Results from select runs of the swamp water mosquito model										
Run	Years	TDD_e	Aquatic T_e	TDD_o	Adult T_o	b	Forcing	Correlation (r)	7-Day smoothed correlation (r)	7-Day smoothed RMS error
1	1986–1990	170	7	100	7	35	T, E	0.42	0.75	16.93
2	1984–1998	170	7	100	7	35	T, E	0.34	0.56	15.84
3	1984–1998	170	7	100	7	35	T, 1000	0.16	0.31	17.71
4	1984–1998	170	7	100	7	35	24, E	0.27	0.34	17.51

Parameter values are listed. Carrying capacity, E, is either derived from Eq. (8) or set to 1000 (Run 3); temperature is either from the measured record or a constant 24 °C (Run 4). Run 1 is the best-fit model for 1986–1990. Run 2 is the best-fit model for 1984–1998. Best-fit models are established based on correlation and RMS error analysis with the New Jersey light trap collection data.
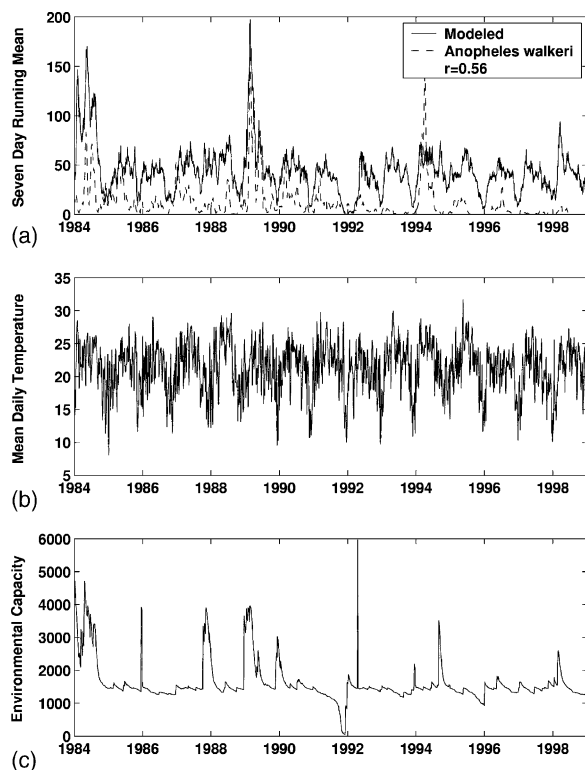
Fig. 8 – (a) Model and measured host-seeking (biting) *Anopheles walkeri*. The model simulation is Run 2, as listed in Table 2. (b) Concurrent mean daily temperature; (c) environmental capacity, *E*.

5. Discussion

We have presented a swamp water mosquito population model that is driven by habitat availability as simulated by a dynamic hydrology model and measured temperature. In doing so, environmental capacity and temperature are not treated as simple harmonic patterns, but as functions with true temporal heterogeneity. Mosquito model simulations were compared to light trap collections of the swamp water mosquito *Anoph. walkeri*. Linear correlation of the modeled and measured populations suggests that some of *Anoph. walkeri* population dynamics are determined by variable environmental capacity, which is a function of hydrologic conditions, and temperature, which affects developmental rates. Determination of population dynamics by the former effect is consistent with findings for theoretical populations with oscillatory carrying capacity and large inherent growth rates (Cushing, 1986). Mosquitoes have a high reproductive rate and can rapidly respond to the vagaries of their changing physical environment. This permits exploitation of these changes and is also consistent with the argument of McArthur and Wilson (1967) that strongly varying environments favor *r*-selected organisms.

Within the mosquito population model, warmer and wetter conditions favor increased *Anoph. walkeri* abundance. The success of the model suggests that a composite index of temperature and modeled surface wetness might crudely capture

Anoph. walkeri population variability. However, simple regression models using modeled hydrology do not capture the population dynamics of the Great Swamp *Anoph. walkeri* record (Shaman et al., 2002) as well as the mosquito population model presented here, nor does multiple regression with both modeled hydrology and temperature (not shown). A better statistical model is established with logistic regression, which is able to estimate likelihoods of high mosquito abundance (but not actual numbers) using modeled hydrology. This relationship is the basis for our estimate of mosquito population sensitivity to hydrologic variability (Eq. (8)).

As presented, the model does fail to capture much of the collected population dynamics from 1993 to 1998, and in particular misses the population spike in 1994. These failures may be due to shortcomings in the population model or could stem from misrepresentation of surface wetness conditions by the hydrology model. The latter explanation is a very real possibility. For instance, while there is a wetting event in 1994 (Fig. 7c), it is not as prolonged as the wetting event occurring in 1989. Wetting of the land surface is highly dependent on patterns of precipitation. At the New Jersey site, where the mosquito collections were taken, there was no available local record of rainfall; instead rainfall data from Allentown, PA, 80 km west, were used to force the hydrology model (for details, see Shaman et al., 2002). These Pennsylvania data should capture regional synoptic rainfall variability at the New Jersey site, but local summertime convective storms may be missed. Consequently, local New Jersey wetting events may be missed or exaggerated, which in turn would lead to mosquito population misrepresentation. In the future, local rainfall measurement should be used to force the hydrology model. Unfortunately, such data were not available for the present study.

There are many ways in which our mosquito population model could possibly be improved. The derivation of environmental capacity, *E*, based on the ILW, though logical as is, could be calculated differently. Alternatively, the effects of this environmental capacity could be implemented differently within the model. In this study, *E* was applied uniformly across all larval cohorts and once per day. Alternatively, reductions of population size based on *E* could be applied to favor certain larval cohorts should they have a competitive advantage in limited habitat conditions over their differently aged conspecifics. To better enable this, the egg, larval and pupal stages might have to be modeled individually.

Other changes might include use of a different equation for mortality as a function of temperature (Eq. (4)). In addition, the present model does not account for overwintering or mosquito dispersal, nor does it synchronize oviposition in response to rainfall or humidity fluctuations. These effects should be incorporated into future modeling efforts.

Within the scope of our current findings, the modeled and measured populations were statistically significantly correlated. However, because the environment (i.e. breeding habitat availability) is variable and the population itself probably oscillates, due to density-dependent factors, non-linear interactions could result from this variability (Nisbet and Gurney, 1976). Our analysis of the modeled and observed populations in the present work has been linear. Future study might analyze the non-linear dynamics of the measured and modeled

populations, such as the recent analyses of insect populations reared in controlled laboratory settings (Costantino et al., 1995, 1998; Dennis et al., 1997).

Our use of simulated breeding habitat availability (a density-independent effect) does not obviate consideration of host–pathogen or other density-dependent effects, but rather offers an additional approach for modeling insect populations. Recent research has shown that density-dependent effects, such as host–pathogen interactions, are unlikely to describe fully the observed variability of insect populations (Vezina and Peterman, 1985; Bowers et al., 1993; Briggs and Godfray, 1996). Swamp water mosquito population dynamics are most likely the consequence of a combination of both density-independent and density-dependent factors, as suggested by May (1986).

The strategy presented here, which uses environmental variability to constrain better model population dynamics, could be incorporated into other population model structures, including simple and matrix population models (e.g. Jensen and Miller, 2004; Federico and Canziani, 2005), metapopulation models (Levins, 1969; Keeling and Gilligan, 2000) and individual-based models (Jaworska et al., 1997; Keeling, 2002; Ovaskainen and Hanski, 2004). Density-independent effects need not be restricted to hydrology but could include both physical and chemical variability, due to climate, weather, rates of weathering and sedimentation, ocean transport, etc. The validity of incorporating any of these density-independent environmental variabilities into a population model structure would depend on the species and system being simulated, their sensitivity to environmental variability, whether this sensitivity can be accurately quantified, and whether the environmental variability itself can be accurately measured or simulated.

A mosquito population model such as the one presented here might prove effective for simulating and predicting swamp water malarial vectors, such as *Anopheles funestus*. It also might be adapted to simulate flood water species, such *Aedes vexans* or *Anopheles gambiae*. Other organisms dependent on fresh water habitat availability could also be modeled. Ultimately, we would like to combine this model with a vector-borne disease or epidemiologic model.

Acknowledgements

Appendix A

We present the derivation of the fixed point solution. With a constant temperature of 24 °C there is a constant mortality rate, i.e. Eq. (2) is:

$$r = \frac{1}{-4.4 + 1.31 \times 24 - 0.03 \times 24^2} = 0.1025$$

In addition, with the parameters TDD_e and TDD_o set to 100 °C, and T_e and T_o set to 14 °C, a temperature of 24 °C implies that all cohorts will emerge as adults on Day 10, reproduce on Days 20 and 30 and die (before reproducing) on Day 40. For these parameters, the number of new larvae equals the reproductive rate, b, times the total number of reproducing adults (cohorts born 20 and 30 days prior), i.e.:

$$\Gamma(t, t_0) = b(N(t, t_{-20}) + N(t, t_{-30})) \tag{A.1}$$

The number of reproducing adults equals the total number of larvae born 20 and 30 days prior times the cumulative mortality, i.e.:

$$N(t, t_{-20}) = \Gamma(t - 20, t_{-20}) \times \exp(-r \times 20) \\ N(t, t_{-30}) = \Gamma(t - 30, t_{-30}) \times \exp(-r \times 30) \tag{A.2}$$

For a fixed point solution to exist there must be equal birth and death such that there is a constant population. We can substitute (A.2) into (A.1) and use the fact that for a constant population $\Gamma(t, t_0) = \Gamma(t - 20, t_{-20}) = \Gamma(t - 30, t_{-30})$ so that:

$$\Gamma(t, t_0) = b\Gamma(t, t_0)(\exp(-r \times 20) + \exp(-r \times 30)) \tag{A3}$$

or

$$b = \frac{1}{\exp(-r \times 20) + \exp(-r \times 30)} \tag{A.4}$$

For $r = -0.1025$, $b = 5.7114$. Thus, with TDD_e and TDD_o set to 100 °C, T_e and T_o set to 14, $T = 24$ °C and $b = 5.7114$ the population exists in steady-state.

REFERENCES

Bowers, R.G., Begon, M., Hodgkinson, D.E., 1993. Host–pathogen poopulation-cycles in forest insects—lessons from simple models reconsidered. Oikos 67, 529–538.

Briggs, C.J., Godfray, H.C.J., 1996. The dynamics of insect–pathogen interactions in seasonal environments. Theor. Popul. Biol. 50, 149–177.

Craig, M.H., Snow, R.W., leSueur, D., 1999. A climate-based distribution model of malaria transmission in sub-Saharan Africa. Parasitol. Today 15, 105.

Costantino, R.F., Cushing, J.M., Dennis, B., Desharnais, R.A., 1995. Experimentally induced transitions in the dynamic behavior of insect populations. Nature 375, 227–230.

Costantino, R.F., Cushing, J.M., Dennis, B., Desharnais, R.A., Henson, S.M., 1998. Resonant population cycles in temporally fluctuating habitats. Bull. Math. Biol. 60, 247–273.

Cushing, J.M., 1986. Oscillatory population growth in periodic environments. Theor. Popoul. Biol. 30, 289–308.

Dennis, B., Desharnais, R.A., Cushing, J.M., Costantino, R.F., 1997. Transitions in population dynamics: equilibria to periodic cycles to aperiodic cycles. J. Anim. Ecol. 66, 704–729.

Federico, P., Canziani, G.A., 2005. Modeling the population dynamics of capybara *Hydrochaeris hydrochaeris*: a first step towards a management plan. Ecol. Model. 186, 111–121.

Jaworska, J.S., Rose, K.A., Brenkert, A.L., 1997. Individual-based modeling of PCBs effects on young-of-the-year largemouth bass in southeastern USA reservoira. Ecol. Model. 99, 113–135.

Jensen, A.L., Miller, D.H., 2004. Modeling emigration of wolves from a wilderness area into adjacent agricultural regions. Ecol. Model. 175, 115–120.

Keeling, M.J., 2002. Using individual-based simulations to test the Levins metapopulation paradigm. J. Anim. Ecol., 270–279.

Keeling, M.J., Gilligan, C.A., 2000. Bubonic plague: a metapopulation model of a zoonosis. Proc. R. Soc. Lond. B 267, 2219–2230.

Kettle, D.S., 1995. Medical and Veterinary Entomology, second ed. CAB International.

Levins, R., 1969. Some demographic and genetic consequences of environmental heterogeneity for biological control. Bull. Entomol. Soc. Am. 15, 237–240.

Martens, W.J.M., 1997. Health Impacts of Climate Change and Ozone Depletion: an Eco-epidemiological Modelling Approach. Maastricht University.

May, R.M., 1986. When two and two do not make four: nonlinear phenomena in ecology. Proc. R. Soc. Lond. B 228, 241–266.

McArthur, R., Wilson, E.O., 1967. The Theory of Island Biogeography. Princeton University Press.

Nisbet, R.M., Gurney, W.S.C., 1976. Population dynamics in a periodically varying environment. J. Theor. Biol. 56, 459–475.

Ovaskainen, O., Hanski, I., 2004. From individual behavior to metapopulation dynamics: unifying the patchy population and classic metapopulation models. Am. Nat. 164, 364–377.

Shaman, J., Stieglitz, M., Stark, C., Le Blancq, S., Cane, M., 2002. Predicting flood and swampwater mosquito abundances using a dynamic hydrology model. Emerg. Infect. Dis. 8, 6–13.

Stieglitz, M., Rind, D., Famiglietti, J., Rosenzweig, C., 1997. An efficient approach to modeling the topographic control of surface hydrology for regional and global climate modeling. J. Clim. 10, 118–137.

Vezina, A., Peterman, R.M., 1985. Tests of the role of a nuclear polyhedrosis-virus in the population dynamics of its host, Douglas-Fir Tussock moth, *Orgyia-pseudotsugata* (Lepidoptera: Lymantriidae). Oecologia 67, 260–266.